Shaping and control of polychromatic light in nonlinear photonic lattices

Andrey A. Sukhorukov, Dragomir N. Neshev, and Yuri S. Kivshar

Center for Ultra-high bandwidth Devices for Optical Systems (CUDOS), Nonlinear Physics Center, Research School of Physical Sciences and Engineering, Australian National University, Canberra ACT 0200, Australia

Abstract: We overview our recent results on spatio-spectral control, diffraction management, broadband switching, and self-trapping of polychromatic light in periodic photonic lattices in the form of rainbow gap solitons, polychromatic surface waves, and multigap color breathers. We show that an interplay of wave scattering from a periodic structure and interaction of multiple colors in media with slow nonlinear response can be used to selectively separate or combine different spectral components. We use an array of optical waveguides fabricated in a $LiNbO_3$ crystal to actively control the output spectrum of the supercontinuum radiation and generate polychromatic gap solitons through a sharp transition from spatial separation of spectral components to the simultaneous spatio-spectral localization of supercontinuum light. We also show that by introducing specially optimized periodic bending of waveguides in the longitudinal direction, one can manage the strength and type of diffraction in an ultra-broad spectral region and, in particular, realize the multicolor Talbot effect.

OCIS codes: (190.4420) Nonlinear optics, transverse effects in; (190.5530) Nonlinear optics: Pulse propagation and solitons; (190.5940) Self-action effects.

References and links

1. J. K. Ranka, R. S. Windeler, and A. J. Stentz, "Visible continuum generation in air-silica microstructure optical fibers with anomalous dispersion at 800 nm," Opt. Lett. **25,** 25–27 (2000).
2. P. St. J. Russell, "Photonic crystal fibers," Science **299,** 358–362 (2003).
3. J. M. Dudley, G. Genty, and S. Coen, "Supercontinuum generation in photonic crystal fiber," Rev. Mod. Phys. **78,** 1135–1184 (2006).
4. T. Udem, R. Holzwarth, and T. W. Hansch, "Optical frequency metrology," Nature **416,** 233–237 (2002).
5. A. M. Zheltikov, "Let there be white light: supercontinuum generation by ultrashort laser pulses," Usp. Fiz. Nauk **176,** 623–649 (2006) (in Russian) [English translation: Phys. Usp. **49,** 605–628 (2006)].
6. B. Povazay, K. Bizheva, A. Unterhuber, B. Hermann, H. Sattmann, A. F. Fercher, W. Drexler, A. Apolonski, W. J. Wadsworth, J. C. Knight, P. St. J. Russell, M. Vetterlein, and E. Scherzer, "Submicrometer axial resolution optical coherence tomography," Opt. Lett. **27,** 1800–1802 (2002).
7. M. H. Qi, E. Lidorikis, P. T. Rakich, S. G. Johnson, J. D. Joannopoulos, E. P. Ippen, and H. I. Smith, "A three-dimensional optical photonic crystal with designed point defects," Nature **429,** 538–542 (2004).
8. M. Balu, J. Hales, D. J. Hagan, and E. W. Van Stryland, "Dispersion of nonlinear refraction and two-photon absorption using a white-light continuum Z-scan," Opt. Express **13,** 3594–3599 (2005), http://www.opticsinfobase.org/abstract.cfm?URI=oe-13-10-3594.
9. J. D. Joannopoulos, R. D. Meade, and J. N. Winn, *Photonic Crystals: Molding the Flow of Light* (Princeton University Press, Princeton, 1995).
10. D. N. Christodoulides and R. I. Joseph, "Discrete self-focusing in nonlinear arrays of coupled wave-guides," Opt. Lett. **13,** 794–796 (1988).
11. H. S. Eisenberg, Y. Silberberg, R. Morandotti, A. R. Boyd, and J. S. Aitchison, "Discrete spatial optical solitons in waveguide arrays," Phys. Rev. Lett. **81,** 3383–3386 (1998).

#84756 - $15.00 USD Received 2 Jul 2007; revised 7 Sep 2007; accepted 7 Sep 2007; published 26 Sep 2007

12. J. W. Fleischer, T. Carmon, M. Segev, N. K. Efremidis, and D. N. Christodoulides, "Observation of discrete solitons in optically induced real time waveguide arrays," Phys. Rev. Lett. **90,** 023902–4 (2003).
13. D. Neshev, E. Ostrovskaya, Y. Kivshar, and W. Krolikowski, "Spatial solitons in optically induced gratings," Opt. Lett. **28,** 710–712 (2003).
14. D. N. Christodoulides, F. Lederer, and Y. Silberberg, "Discretizing light behaviour in linear and nonlinear waveguide lattices," Nature **424,** 817–823 (2003).
15. A. A. Sukhorukov, Yu. S. Kivshar, H. S. Eisenberg, and Y. Silberberg, "Spatial optical solitons in waveguide arrays," IEEE J. Quantum Electron. **39,** 31–50 (2003).
16. A. Fratalocchi, G. Assanto, K. A. Brzdakiewicz, and M. A. Karpierz, "Discrete propagation and spatial solitons in nematic liquid crystals," Opt. Lett. **29,** 1530–1532 (2004).
17. R. Iwanow, R. Schiek, G. I. Stegeman, T. Pertsch, F. Lederer, Y. Min, and W. Sohler, "Observation of discrete quadratic solitons," Phys. Rev. Lett. **93,** 113902–4 (2004).
18. F. Chen, M. Stepic, C. E. Ruter, D. Runde, D. Kip, V. Shandarov, O. Manela, and M. Segev, "Discrete diffraction and spatial gap solitons in photovoltaic $LiNbO_3$ waveguide arrays," Opt. Express **13,** 4314–4324 (2005), http://www.opticsinfobase.org/abstract.cfm?URI=oe-13-11-4314.
19. J. W. Fleischer, G. Bartal, O. Cohen, T. Schwartz, O. Manela, B. Freedman, M. Segev, H. Buljan, and N. K. Efremidis, "Spatial photonics in nonlinear waveguide arrays," Opt. Express **13,** 1780–1796 (2005), http://www.opticsinfobase.org/abstract.cfm?URI=oe-13-6-1780.
20. A. Szameit, D. Blomer, J. Burghoff, T. Schreiber, T. Pertsch, S. Nolte, A. Tunnermann, and F. Lederer, "Discrete nonlinear localization in femtosecond laser written waveguides in fused silica," Opt. Express **13,** 10552–10557 (2005), http://www.opticsinfobase.org/abstract.cfm?URI=oe-13-26-10552.
21. M. Matuszewski, C. R. Rosberg, D. N. Neshev, A. A. Sukhorukov, A. Mitchell, M. Trippenbach, M. W. Austin, W. Krolikowski, and Yu. S. Kivshar, "Crossover from self-defocusing to discrete trapping in nonlinear waveguide arrays," Opt. Express **14,** 254–259 (2006), http://www.opticsinfobase.org/abstract.cfm?URI=oe-14-1-254.
22. A. Szameit, D. Blomer, J. Burghoff, T. Pertsch, S. Nolte, and A. Tunnermann, "Hexagonal waveguide arrays written with fs-laser pulses," Appl. Phys. B **82,** 507–512 (2006).
23. D. N. Neshev, A. A. Sukhorukov, W. Krolikowski, and Yu. S. Kivshar, "Nonlinear optics and light localization in periodic photonic lattices," J. Nonlinear Opt. Phys. Mater. **16,** 1–25 (2007).
24. K. Motzek, A. A. Sukhorukov, Yu. S. Kivshar, and F. Kaiser, "Polychromatic multigap solitons in nonlinear photonic lattices," In *Nonlinear Guided Waves and Their Applications*, Postconference ed. OSA p. WD25 (Optical Society of America, Washington DC, 2005).
25. K. Motzek, A. A. Sukhorukov, and Yu. S. Kivshar, "Self-trapping of polychromatic light in nonlinear periodic photonic structures," Opt. Express **14,** 9873–9878 (2006), http://www.opticsinfobase.org/abstract.cfm?URI=oe-14-21-9873.
26. K. Motzek, A. A. Sukhorukov, and Yu. S. Kivshar, "Polychromatic interface solitons in nonlinear photonic lattices," Opt. Lett. **31,** 3125–3127 (2006).
27. A. A. Sukhorukov, D. N. Neshev, A. Dreischuh, R. Fischer, S. Ha, W. Krolikowski, J. Bolger, A. Mitchell, B. J. Eggleton, and Yu. S. Kivshar, "Polychromatic nonlinear surface modes generated by supercontinuum light," Opt. Express **14,** 11265–11270 (2006), http://www.opticsinfobase.org/abstract.cfm?URI=oe-14-23-11265.
28. I. L. Garanovich, A. A. Sukhorukov, and Yu. S. Kivshar, "Broadband diffraction management and self-collimation of white light in photonic lattices," Phys. Rev. E **74,** 066609–4 (2006).
29. A. A. Sukhorukov, D. Neshev, A. Dreischuh, R. Fischer, S. Ha, W. Krolikowski, J. Bolger, B. J. Eggleton, A. Mitchell, M. W. Austin, and Yu. S. Kivshar, "Polychromatic gap solitons and breathers in nonlinear waveguide arrays," In *Nonlinear Photonics Topical Meeting*, Conference ed. OSA p. JMB5 (Optical Society of America, Washington DC, 2007).
30. D. N. Neshev, A. A. Sukhorukov, A. Dreischuh, R. Fischer, S. Ha, J. Bolger, L. Bui, W. Krolikowski, B. J. Eggleton, A. Mitchell, M. W. Austin, and Yu. S. Kivshar, "Nonlinear spectral-spatial control and localization of supercontinuum radiation," Phys. Rev. Lett. 99 (2007), in press.
31. I. L. Garanovich, A. Szameit, A. A. Sukhorukov, T. Pertsch, W. Krolikowski, S. Nolte, D. Neshev, A. Tuennermann, and Yu. S. Kivshar, "Diffraction control in periodically curved two-dimensional waveguide arrays," Opt. Express **15,** 9737–9747 (2007), http://www.opticsinfobase.org/abstract.cfm?URI=oe-15-15-9737.
32. A. A. Sukhorukov, D. N. Neshev, A. Dreischuh, R. Fischer, W. Krolikowski, J. Bolger, B. J. Eggleton, L. Bui, A. Mitchell, and Yu.S. Kivshar, "Observation of polychromatic gap solitons," submitted for publication (2007).
33. A. L. Jones, "Coupling of optical fibers and scattering in fibers," J. Opt. Soc. Am. **55,** 261 (1965).
34. S. Somekh, E. Garmire, A. Yariv, H. L. Garvin, and R. G. Hunsperger, "Channel optical waveguide directional couplers," Appl. Phys. Lett. **22,** 46–47 (1973).
35. R. Iwanow, D. A. May Arrioja, D. N. Christodoulides, G. I. Stegeman, Y. Min, and W. Sohler, "Discrete Talbot effect in waveguide arrays," Phys. Rev. Lett. **95,** 053902–4 (2005).
36. P. Yeh, *Optical Waves in Layered Media* (John Wiley & Sons, New York, 1988).
37. P. St. J. Russell, T. A. Birks, and F. D. Lloyd Lucas, "Photonic Bloch waves and photonic band gaps," in *Confined Electrons and Photons*, E. Burstein and C. Weisbuch, eds., (Plenum, New York, 1995), pp. 585–633.
38. D. N. Christodoulides, S. R. Singh, M. I. Carvalho, and M. Segev, "Incoherently coupled soliton pairs in biased

#84756 - $15.00 USD Received 2 Jul 2007; revised 7 Sep 2007; accepted 7 Sep 2007; published 26 Sep 2007

photorefractive crystals," Appl. Phys. Lett. **68,** 1763–1765 (1996).
39. M. Mitchell and M. Segev, "Self-trapping of incoherent white light," Nature **387,** 880–883 (1997).
40. H. Buljan, T. Schwartz, M. Segev, M. Soljacic, and D. N. Christodoulides, "Polychromatic partially spatially incoherent solitons in a noninstantaneous Kerr nonlinear medium," J. Opt. Soc. Am. B **21,** 397–404 (2004).
41. A. Alberucci, M. Peccianti, G. Assanto, A. Dyadyusha, and M. Kaczmarek, "Two-color vector solitons in nonlocal media," Phys. Rev. Lett. **97,** 153903–4 (2006).
42. A. B. Fedotov, A. N. Naumov, I. Bugar, D. Chorvat, D. A. Sidorov Biryukov, D. Chorvat, and A. M. Zheltikov, "Supercontinuum generation in photonic-molecule modes of microstructure fibers," IEEE J. Sel. Top. Quantum Electron. **8,** 665–674 (2002).
43. A. B. Fedotov, I. Bugar, A. N. Naumov, D. Chorvat, Jr, D. A. Sidorov Biryukov, D. Chorvat, and A. M. Zheltikov, "Light confinement and supercontinuum generation switching in photonic-molecule modes of a microstructure fiber," Pis'ma Zh. Éksp. Teor. Fiz. **75,** 374–378 (2002) (in Russian) [English translation: JETP Lett. **75,** 304–308 (2002)].
44. A. Betlej, S. Suntsov, K. G. Makris, L. Jankovic, D. N. Christodoulides, G. I. Stegeman, J. Fini, R. T. Bise, and J. DiGiovanni, "All-optical switching and multifrequency generation in a dual-core photonic crystal fiber," Opt. Lett. **31,** 1480–1482 (2006).
45. G. C. Valley, M. Segev, B. Crosignani, A. Yariv, M. M. Fejer, and M. C. Bashaw, "Dark and bright photovoltaic spatial solitons," Phys. Rev. A **50,** R4457–R4460 (1994).
46. Z. Y. Xu, Y. V. Kartashov, and L. Torner, "Gap solitons supported by optical lattices in photorefractive crystals with asymmetric nonlocality," Opt. Lett. **31,** 2027–2029 (2006).
47. R. R. Shah, D. M. Kim, T. A. Rabson, and F. K. Tittel, "Characterisation of iron-doped lithium niobate for holographic storage applications," J. Appl. Phys. **47,** 5421–5431 (1976).
48. F. Jermann, M. Simon, and E. Kratzig, "Photorefractive properties of congruent and stoichiometric lithium niobate at high light intensities," J. Opt. Soc. Am. B **12,** 2066–2070 (1995).
49. R. Pezer, H. Buljan, G. Bartal, M. Segev, and J. W. Fleischer, "Incoherent white-light solitons in nonlinear periodic lattices," Phys. Rev. E **73,** 056608–9 (2006).
50. D. Mandelik, H. S. Eisenberg, Y. Silberberg, R. Morandotti, and J. S. Aitchison, "Observation of mutually trapped multiband optical breathers in waveguide arrays," Phys. Rev. Lett. **90,** 253902–4 (2003).
51. A. Fratalocchi, G. Assanto, K. A. Brzdakiewicz, and M. A. Karpierz, "Optical multiband vector breathers in tunable waveguide arrays," Opt. Lett. **30,** 174–176 (2005).
52. A. Fratalocchi, G. Assanto, K. A. Brzdakiewicz, and M. A. Karpierz, "Discrete light propagation and self-trapping in liquid crystals," Opt. Express **13,** 1808–1815 (2005), http://www.opticsinfobase.org/abstract.cfm?URI=oe-13-6-1808.
53. A. Ashkin, G. D. Boyd, J. M. Dziedzic, R. G. Smith, A. A. Ballman, J. J. Levinstein, and K. Nassau, "Optically-induced refractive index inhomogeneities in $LiNbO_3$ and $LiTaO_3$," Appl. Phys. Lett. **9,** 72–74 (1966).
54. D. Kip, "Photorefractive waveguides in oxide crystals: fabrication, properties, and applications," Appl. Phys. B **67,** 131–150 (1998).
55. G. I. Stegeman and M. Segev, "Optical spatial solitons and their interactions: Universality and diversity," Science **286,** 1518–1523 (1999).
56. Yu. S. Kivshar and G. P. Agrawal, *Optical Solitons: From Fibers to Photonic Crystals* (Academic Press, San Diego, 2003).
57. A. Guo, M. Henry, G. J. Salamo, M. Segev, and G. L. Wood, "Fixing multiple waveguides induced by photorefractive solitons: directional couplers and beam splitters," Opt. Lett. **26,** 1274–1276 (2001).
58. P. Zhang, D. X. Yang, J. L. Zhao, and M. R. Wang, "Photo-written waveguides in iron-doped lithium niobate crystal employing binary optical masks," Opt. Eng. **45,** 074603–7 (2006).
59. P. Yeh, A. Yariv, and C. S. Hong, "Electromagnetic propagation in periodic stratified media .1. General theory," J. Opt. Soc. Am. **67,** 423–438 (1977).
60. P. Yeh, A. Yariv, and A. Y. Cho, "Optical surface-waves in periodic layered media," Appl. Phys. Lett. **32,** 104–105 (1978).
61. K. G. Makris, S. Suntsov, D. N. Christodoulides, G. I. Stegeman, and A. Hache, "Discrete surface solitons," Opt. Lett. **30,** 2466–2468 (2005).
62. S. Longhi, "Tunneling escape in optical waveguide arrays with a boundary defect," Phys. Rev. E **74,** 026602–9 (2006).
63. K. G. Makris, J. Hudock, D. N. Christodoulides, G. I. Stegeman, O. Manela, and M. Segev, "Surface lattice solitons," Opt. Lett. **31,** 2774–2776 (2006).
64. M. I. Molina and Yu. S. Kivshar, "Interface localized modes and hybrid lattice solitons in waveguide arrays," Phys. Lett. A **362,** 280–282 (2007).
65. S. Suntsov, K. G. Makris, D. N. Christodoulides, G. I. Stegeman, R. Morandotti, M. Volatier, V. Aimez, R. Ares, C. E. Ruter, and D. Kip, "Optical modes at the interface between two dissimilar discrete meta-materials," Opt. Express **15,** 4663–4670 (2007), http://www.opticsinfobase.org/abstract.cfm?URI=oe-15-8-4663.
66. S. Suntsov, K. G. Makris, D. N. Christodoulides, G. I. Stegeman, A. Hache, R. Morandotti, H. Yang, G. Salamo, and M. Sorel, "Observation of discrete surface solitons," Phys. Rev. Lett. **96,** 063901–4 (2006).

#84756 - $15.00 USD Received 2 Jul 2007; revised 7 Sep 2007; accepted 7 Sep 2007; published 26 Sep 2007

67. Y. V. Kartashov, V. A. Vysloukh, and L. Torner, "Surface gap solitons," Phys. Rev. Lett. **96,** 073901–4 (2006).
68. G. A. Siviloglou, K. G. Makris, R. Iwanow, R. Schiek, D. N. Christodoulides, G. I. Stegeman, Y. Min, and W. Sohler, "Observation of discrete quadratic surface solitons," Opt. Express **14,** 5508–5516 (2006), http://www.opticsinfobase.org/abstract.cfm?URI=oe-14-12-5508.
69. E. Smirnov, M. Stepic, C. E. Ruter, D. Kip, and V. Shandarov, "Observation of staggered surface solitary waves in one-dimensional waveguide arrays," Opt. Lett. **31,** 2338–2340 (2006).
70. C. R. Rosberg, D. N. Neshev, W. Krolikowski, A. Mitchell, R. A. Vicencio, M. I. Molina, and Yu. S. Kivshar, "Observation of surface gap solitons in semi-infinite waveguide arrays," Phys. Rev. Lett. **97,** 083901–4 (2006).
71. I. L. Garanovich, A. A. Sukhorukov, Yu. S. Kivshar, and M. Molina, "Surface multi-gap vector solitons," Opt. Express **14,** 4780–4785 (2006), http://www.opticsinfobase.org/abstract.cfm?URI=oe-14-11-4780.
72. Y. V. Kartashov, F. W. Ye, and L. Torner, "Vector mixed-gap surface solitons," Opt. Express **14,** 4808–4814 (2006), http://www.opticsinfobase.org/abstract.cfm?URI=oe-14-11-4808.
73. M. Born and E. Wolf, *Principles of optics: electromagnetic theory of propagation, interference and diffraction of light* (Pergamon Press, London, 1959).
74. H. S. Eisenberg, Y. Silberberg, R. Morandotti, and J. S. Aitchison, "Diffraction management," Phys. Rev. Lett. **85,** 1863–1866 (2000).
75. M. J. Ablowitz and Z. H. Musslimani, "Discrete diffraction managed spatial solitons," Phys. Rev. Lett. **87,** 254102–4 (2001).
76. G. Lenz, R. Parker, M. C. Wanke, and C. M. de Sterke, "Dynamical localization and AC Bloch oscillations in periodic optical waveguide arrays," Opt. Commun. **218,** 87–92 (2003).
77. J. Wan, M. Laforest, C. M. de Sterke, and M. M. Dignam, "Optical filters based on dynamic localization in curved coupled optical waveguides," Opt. Commun. **247,** 353–365 (2005).
78. S. Longhi, M. Marangoni, M. Lobino, R. Ramponi, P. Laporta, E. Cianci, and V. Foglietti, "Observation of dynamic localization in periodically curved waveguide arrays," Phys. Rev. Lett. **96,** 243901–4 (2006).
79. R. Iyer, J. S. Aitchison, J. Wan, M. M. Dignam, and C. M. de Sterke, "Exact dynamic localization in curved AlGaAs optical waveguide arrays," Opt. Express **15,** 3212–3223 (2007), http://www.opticsinfobase.org/abstract.cfm?URI=oe-15-6-3212.
80. I. L. Garanovich and A. A. Sukhorukov, "Nonlinear directional coupler for polychromatic light," Opt. Lett. **32,** 475–477 (2007).
81. H. F. Talbot, "Facts relating to optical science," Phil. Mag. **9,** 401–407 (1836).

1. Introduction

Advances in the generation of light with broadband or supercontinuum spectrum in photonic-crystal fibers [1–3] open many new possibilities for a wide range of applications including optical frequency metrology [4], spectroscopy [5], tomography [6], and optical characterization of photonic crystals [7]. Supercontinuum radiation differs significantly from the light emitted by incoherent light sources, combining high coherence, spectral brightness, and excellent focusing properties. Furthermore, its high peak intensity and average power enable enhanced light-matter interactions in the nonlinear regime [8]. In recent years, efficient approaches have been developed for the manipulation of temporal and spectral characteristics of supercontinuum generated in photonic crystal fibers (PCFs) [2]. PCFs allow for engineering of the spectral dispersion and confinement of light through the underlying periodicity of their structure. On the other hand, various applications would benefit from the ability to perform tunable shaping of the supercontinuum light beams in the spatial domain.

The spatial beam manipulation in extended photonic structures is based on the scattering of waves from the refractive index inhomogeneities and their subsequent interference. This is a resonant process, which is sensitive to both the frequency and the propagation angle. In photonic crystals [9] where the refractive index is modulated in the propagation direction on the scale of the optical wavelength, there appear sharp spectral features where the propagation of optical signals is highly sensitive to the wavelength. Another class of periodic structures in the form of waveguide arrays, shown schematically in Fig. 1(a), or photonic lattices [10–23] feature the refractive index modulation in the transverse spatial dimension with the characteristic period of several wavelengths, resembling the periodic cladding of PCFs. In such structures the back-scattering of light is absent and transmission coefficients can approach unity simultaneously for all spectral components. Additionally, the spatial beam propagation in waveguide arrays tends

#84756 - $15.00 USD Received 2 Jul 2007; revised 7 Sep 2007; accepted 7 Sep 2007; published 26 Sep 2007

to change smoothly as the optical wavelength is varied strongly by hundreds of nanometers. These features of photonic-lattice structures make them well suited for the manipulation of polychromatic or supercontinuum light beams.

In this paper, we overview our recent theoretical and experimental results [24–32] on the tunable control of the supercontinuum light beams by employing nonlinear photonic latices. Whereas various approaches for all-optical beam shaping have been previously demonstrated for narrow-band light sources, we reveal novel possibilities for all-optical spatial switching and simultaneous spectral reshaping and localization of supercontinuum light beams. We predict theoretically and demonstrate experimentally that an interplay of wave scattering from a periodic structure and nonlinearity-induced interaction of multiple colors in an array of optical waveguides allows one to selectively separate or combine different spectral components. Additional flexibility is implemented through interaction with induced defects in the structure, where small refractive index change may enable tunable spectral filtering. We also show that in optimized arrays of curved waveguides, it is possible to achieve an efficient diffraction management of polychromatic light and, in particular, realize the multicolor Talbot effect.

The paper is organized as follows. In Sec. 2 we present the basic concepts of polychromatic light propagation in photonic lattices at low light intensity (linear propagation). In Sec. 3 we describe the effect of nonlinear material response on the beam spectral-spatial reshaping with propagation. We show how the collective nonlinear interaction of spectral components in a medium with slow nonlinearity leads to the formation of polychromatic gap solitons and breathers. In Sec. 4 we provide experimental verification of some of our theoretical predictions and demonstrate how the slow defocusing photorefractive nonlinearity in lithium niobate waveguide arrays can be used for tunable all-optical reshaping of supercontinuum light. Sec. 5 describes the ability of surfaces to dramatically alter the propagation of polychromatic light and presents theoretical and experimental results on the formation of polychromatic nonlinear surface states. Finally, in Sec. 6 we describe the possibility for diffraction engineering in an ultra-broad spectral region by introducing periodic bending of waveguides in the longitudinal direction, offering new possibilities for shaping of polychromatic beams and patterns.

2. Polychromatic beam shaping in linear photonic lattices

In this section, we discuss the general features of polychromatic beam diffraction in planar photonic structures with a modulation of the refractive index along the transverse spatial dimension [Fig. 1(a)], such as optically-induced lattices or periodic waveguide arrays [10–23]. The physical mechanism of beam diffraction in such structures is based on the coupling between the modes of neighboring waveguides [14, 33, 34]. When the beam is coupled into a single waveguide at the input, it experiences ‘discrete diffraction’ where most of the light is directed into the wings of the beam. This is in sharp contrast to the diffraction of Gaussian beams in homogeneous materials where the peak intensity remains at the beam center at any propagation distance. The light couples from one waveguide to another due to the spatial overlaps of the waveguide modes. Since the mode profile and confinement depend on the wavelength, the discrete diffraction exhibits spectral dispersion. The mode overlap at neighboring waveguides is usually much stronger for red-shifted components, which therefore diffract faster than their blue counterparts [22,35]. This leads to spatial redistribution of the colors of the polychromatic beam which increases along the propagation direction, see Fig. 1(b). As a result, at the output the red components dominate in the beam wings, while the blue components are dominant in the central region, see Fig. 1(c).

The mathematical modeling of the diffraction process for optical sources with a high degree of spatial coherence, such as supercontinuum light generated in photonic-crystal fibers, can be based on a set of equations for the spatial beam envelopes $A_m(x,z)$ of different frequency

#84756 - $15.00 USD Received 2 Jul 2007; revised 7 Sep 2007; accepted 7 Sep 2007; published 26 Sep 2007

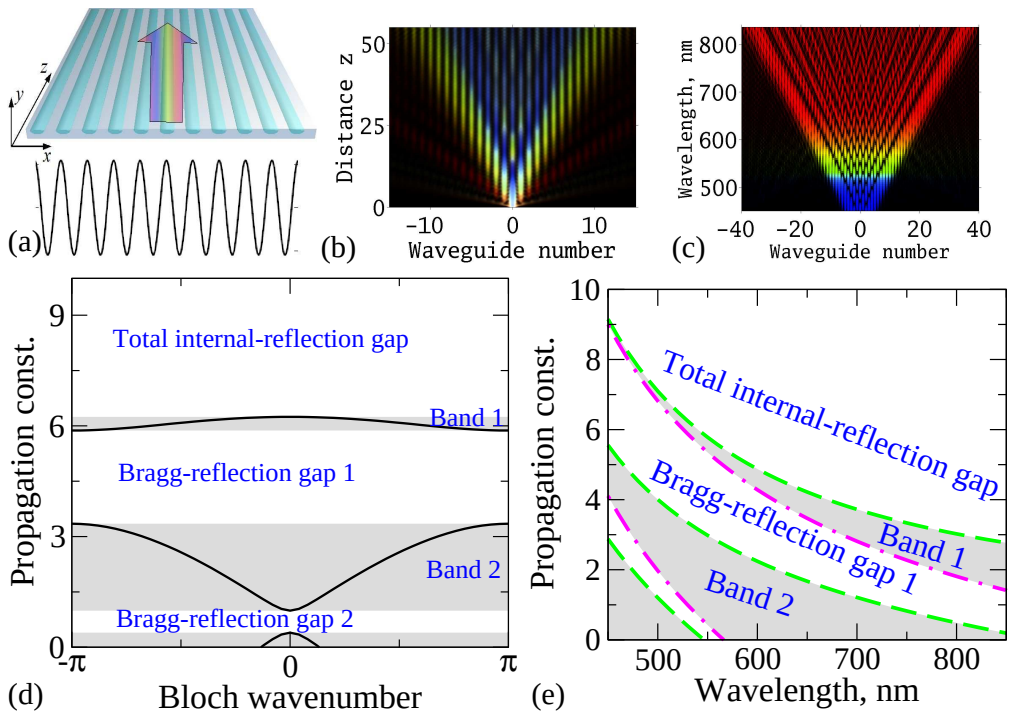

Fig. 1. (a) Schematic of the waveguide array structure (top) and the characteristic transverse refractive index profile (bottom). (b,c) Numerical simulation of polychromatic beam diffraction: (b) real-color image of beam evolution inside the array and (c) the spectrally-resolved output profiles. (d) Bloch-wave dispersion at 530 nm wavelength. (e) Dependence of photonic bands on wavelength. Numerical simulations correspond to the parameters of $LiNbO_3$ waveguide arrays [29, 32], discussed below in Sec. 4.2.

components at vacuum wavelengths λ_m. Since the refractive index contrast in photonic-lattice structures is usually of the order of 10^{-4} to 10^{-2} and we consider the beams propagating at small angles along the lattice, then the general wave equations can be reduced to parabolic equations employing the conventional paraxial approximation [25, 30, 32],

$$i\frac{\partial A_m}{\partial z} + \frac{\lambda_m}{4\pi n_0(\lambda_m)}\frac{\partial^2 A_m}{\partial x^2} + \frac{2\pi}{\lambda_m}\Delta n(x;\lambda_m)A_m = 0, \tag{1}$$

where x and z are the transverse and longitudinal coordinates, respectively, and $n_0(\lambda_m)$ is the background refractive index. The function $\Delta n(x;\lambda_m)$ describes the effective refractive index modulation, which depends on the vertical mode confinement in the planar guiding structure. Since the vertical mode profile changes with wavelength, the dispersion of the effective index modulation is defined by the geometry of photonic structures. For an array of optical waveguides in $LiNbO_3$, the modulation can be accurately described as $\Delta n(x;\lambda) = \Delta n_{\max}(\lambda)\cos^2(\pi x/d)$, where the wavelength dependence of the effective modulation depth $\Delta n_{\max}(\lambda)$ can be calculated numerically or determined by matching the experimentally measured waveguide coupling [30, 32]. Even if the material and geometrical dispersion effects are weak, the beam propagation would still strongly depend on its frequency spectrum [24, 25] since the values of λ_m appear explicitly in Eqs. (1).

Linear propagation of optical beams through a periodic lattice can be fully characterized by decomposing the input profile in a set of spatially extended eigenmodes, called Bloch

#84756 - $15.00 USD Received 2 Jul 2007; revised 7 Sep 2007; accepted 7 Sep 2007; published 26 Sep 2007

waves [36, 37]. The Bloch-wave profiles can be found as solutions of Eqs. (1) in the form $A_m(x,z) = \psi_j(x;\lambda_m)\exp[i\beta_j(K_b;\lambda_m)z + iK_b x/d]$, where $\psi_j(x;\lambda_m)$ has the periodicity of the underlying lattice, $\beta_j(K_b;\lambda_m)$ are the propagation constants, K_b are the normalized Bloch wavenumbers, j is the band number, and d is the lattice period. At each wavelength, the dependencies of longitudinal propagation constant (along z) on the transverse Bloch wavenumber (along x) are periodic, $\beta_j(K_b;\lambda_m) = \beta_j(K_b \pm 2\pi;\lambda_m)$, and are fully characterized by their values in the first Brillouin zone, $-\pi \le K_b \le \pi$. These dependencies have a universal character [9, 36, 37], where the spectrum consists of non-overlapping bands separated by photonic bandgaps, as shown in Fig. 1(d). The position and the width of bands and gaps, however, are strongly sensitive to the wavelength of the light [Fig. 1(e)]. As a result, the spatial beam shaping exhibits frequency dispersion. In particular, the rate of diffraction for broad beams is determined by the curvature of dispersion curves, $\partial^2\beta_j(K_b;\lambda_m)/\partial K_b^2$. For the input beam coupled to a single waveguide, the first band is primarily excited ($j = 1$), and the beam diffraction increases at longer wavelengths where the band gets wider. This conclusion is in full agreement with the physical interpretation presented above using the concept of coupling between waveguide modes.

3. Self-trapping of polychromatic light

An important task of building a nonlinear, reconfigurable photonic device for manipulation of broadband signals requires the ability to tune the spectral transmission in the spatial domain. In this section, we describe an approach to flexible spatial-spectral control of supercontinuum radiation through the effect of nonlinear interaction and selective self-trapping of spectral components inside the individual channels of the waveguide array.

3.1. Collective nonlinear interactions in media with slow nonlinearity

In order to perform spatial switching and reshaping of polychromatic signals without generating or depleting different spectral regions, the coherent four-wave-mixing processes need to be suppressed. This can be achieved in media which nonlinear response is slow with respect to the scale of temporal coherence [38]. This condition is commonly satisfied for photorefractive materials, where the optically-induced refractive index change is defined by the time-averaged light intensity of different spectral components [39, 40]. Similar types of multi-wavelength interactions are also possible in liquid crystals [41]. The slow nonlinearities thus provide a fundamentally different regime compared to dynamics of light with supercontinuum spectrum in multi-core photonic-crystal fibers with fast nonlinear response [42–44], where nonlinearly-induced spatial mode reshaping is inherently accompanied by the spectral transformations.

We model the nonlinear propagation and interaction of all spectral components by including a nonlinearly-induced change of the refractive index into Eqs. (1),

$$i\frac{\partial A_m}{\partial z} + \frac{\lambda_m}{4\pi n_0(\lambda_m)}\frac{\partial^2 A_m}{\partial x^2} + \frac{2\pi}{\lambda_m}\left[\Delta n(x;\lambda_m) + \Delta n_{\rm nl}(x,z)\right]A_m = 0, \tag{2}$$

We take the nonlinear term in the form: $\Delta n_{\rm nl}(x,z) = \gamma M^{-1}\sum_{j=1}^{M}\sigma(\lambda_j)|A_j|^2$, which accounts for photovoltaic defocusing nonlinearity [40, 45] in the regime of weak saturation, where γ is the nonlinear coefficient, and M is the number of frequency components included in numerical modeling. Whereas nonlocality may affect the soliton properties [46], this effect was weak under our experimental conditions [27, 29, 30, 32]. For the $LiNbO_3$ waveguide arrays, the photovoltaic nonlinearity arises due to charge excitations by light absorption and corresponding separation of these charges due to diffusion. The spectral response of this type of nonlinearity depends on the crystal doping and stoichiometry and may vary from crystal to crystal. In general, however, light sensitivity appears in a wide spectral range with a

#84756 - $15.00 USD Received 2 Jul 2007; revised 7 Sep 2007; accepted 7 Sep 2007; published 26 Sep 2007

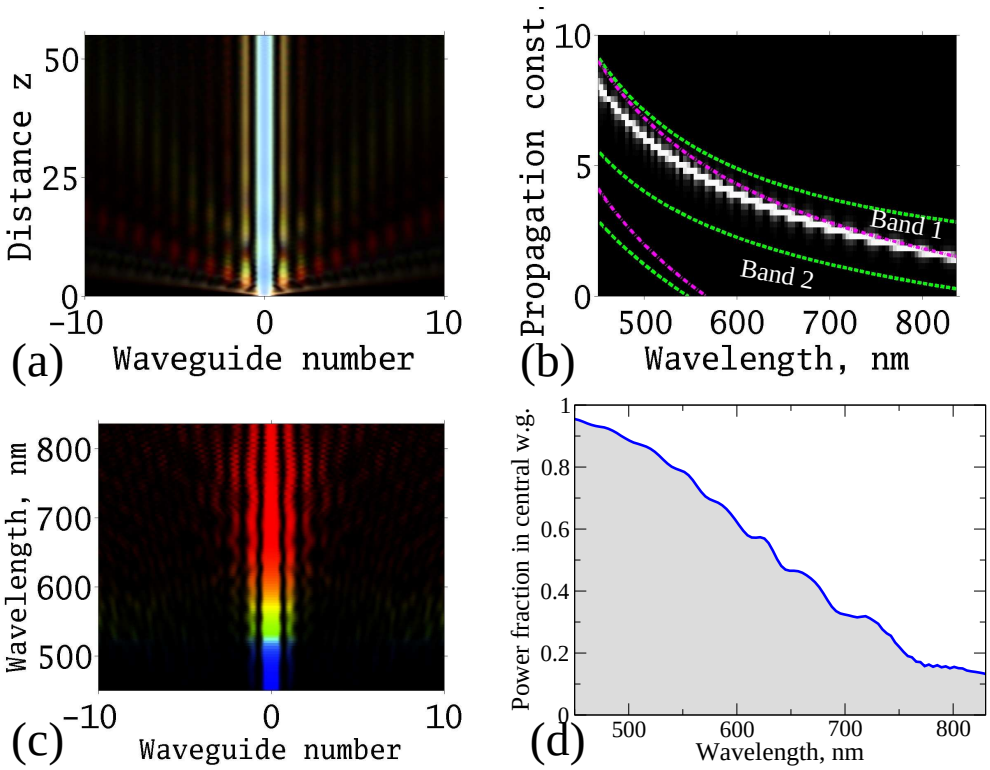

Fig. 2. Numerical modeling of nonlinear beam self-trapping and formation of polychromatic gap soliton [29, 32] based on Eqs. (2) with $M = 100$ and $\gamma = -1$: (a) Soliton excitation inside the waveguide array, (b) Propagation constants vs. the wavelength for the soliton beam, dashed and dashed-dotted lines mark the band edges as indicated in Fig. 1(e). (c) Spectrally resolved output intensity profile. (d) The fraction of output power remaining in the central waveguide for different spectral components.

maximum for the blue spectral components [47], but the sensitivity extends well in the near infra-red region [48]. We approximate the photosensitivity dependence by a Gaussian function $\sigma(\lambda) = \exp[-\log(2)(\lambda - \lambda_b)^2/\lambda_w^2]$ with $\lambda > \lambda_b = 400\,\text{nm}$ and $\lambda_w = 150\,\text{nm}$. Note that by making a transformation $\tilde{A}_m = A_m\sqrt{\sigma(\lambda_m)}$, the sensitivity function can be rescaled to unity, $\widetilde{\sigma}(\lambda_m) = 1$, and therefore the presented results are also directly applicable for other shapes of sign-definite photosensitivity functions.

3.2. *Polychromatic gap solitons*

Multiple frequency components of an optical beam can undergo self-trapping process and propagate in a common direction, when they are coupled together and form a polychromatic spatial soliton. The solitons are self-trapped beams which do not diffract, and their formation was predicted to occur in media with either self-defocusing [24, 25] or self-focusing [49] nonlinearities. The self-focusing nonlinearity can also support polychromatic or white-light solitons in bulk media [39, 40], and we consider below the most intriguing case of polychromatic soliton formation in lattices with defocusing nonlinearity, when localization would not be possible for bulk crystals. The experimental observations of such self-trapping effect are discussed below in Sec. 4.

#84756 - $15.00 USD Received 2 Jul 2007; revised 7 Sep 2007; accepted 7 Sep 2007; published 26 Sep 2007

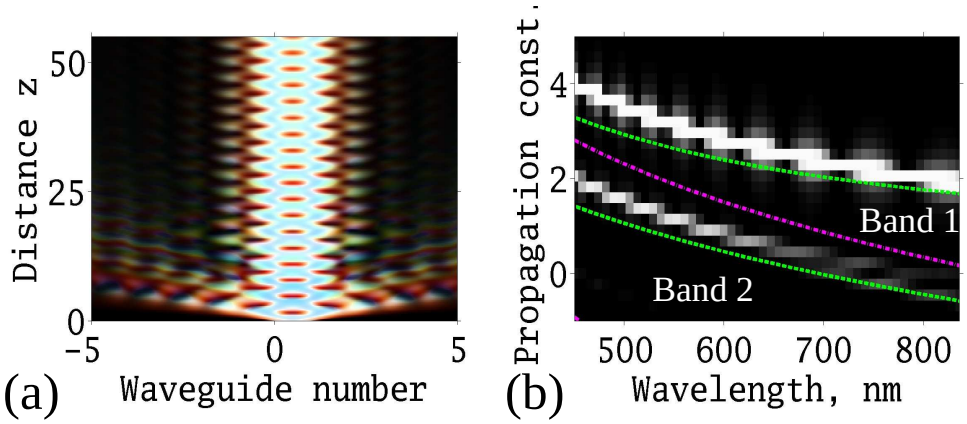

Fig. 3. Example of the numerically calculated polychromatic multigap breather in a photonic lattice with self-focusing nonlinearity ($\gamma = +1$ and $M = 50$). (a) Beam propagation dynamics, and (b) Propagation constants vs. the wavelength, dashed and dashed-dotted lines mark the band edges [29].

The numerical simulations based on the system of equations (2) (with $\gamma = -1$ for defocusing nonlinear response) show that the input beam experiences self-trapping above a critical power level [24, 25, 29, 32]. In this regime, the spectral components become spatially localized and form a polychromatic soliton, which propagates without broadening in the photonic structure, see Fig. 2(a). In order to identify the physical mechanism of beam localization and soliton formation, we calculate the spectrum of the propagation constants, which is presented as density plot (white color correspond to larger amplitudes) in Fig. 2(b). This figure shows that the propagation constants are located inside the Bragg-reflection gap due to the nonlinear decrease of the refractive index at the soliton core, and this allows for the spatial self-trapping. Thus, such self-trapped states can be termed *polychromatic gap solitons*. Note that the spectrum for blue components is shifted deeper inside the gap, whereas the red components have spectra very close to the gap edge. This explains much weaker localization of red components as shown in Figs. 2(c) and (d), and indeed it is seen in Fig. 2(a) that the soliton has a blue center and red tails.

3.3. Crossover from self-trapping to defocusing

The variation of the gap width can have a dramatic effect on self-action of an input beam focused at a single site of a defocusing nonlinear lattice [21], where a sharp crossover from self-trapping to defocusing occurs as the gap becomes narrower. Since the gap-width depends on wavelength as discussed in Sec. 2, both self-focusing and defocusing phenomena may be observed in the same photonic structure depending on the value of the wavelength $\lambda_{\rm cr}$ corresponding to the crossover transition [25]. When $\lambda_{\rm cr}$ is above the optical spectrum, the polychromatic gap solitons may always be excited as discussed in Sec. 3.2. However, in photonic lattices with smaller refractive index contrast, $\lambda_{\rm cr}$ is shifted to lower wavelengths. Then, for particular spectral shapes, the soliton formation is not observed at any power levels when the input beam is coupled to a single waveguide. Importantly, such effects do not occur in lattices with positive or self-focusing nonlinearity [49]. These results underline the importance of proper engineering of photonic-lattice structures and suggest new opportunities for spectrally-sensitive beam shaping.

#84756 - $15.00 USD Received 2 Jul 2007; revised 7 Sep 2007; accepted 7 Sep 2007; published 26 Sep 2007

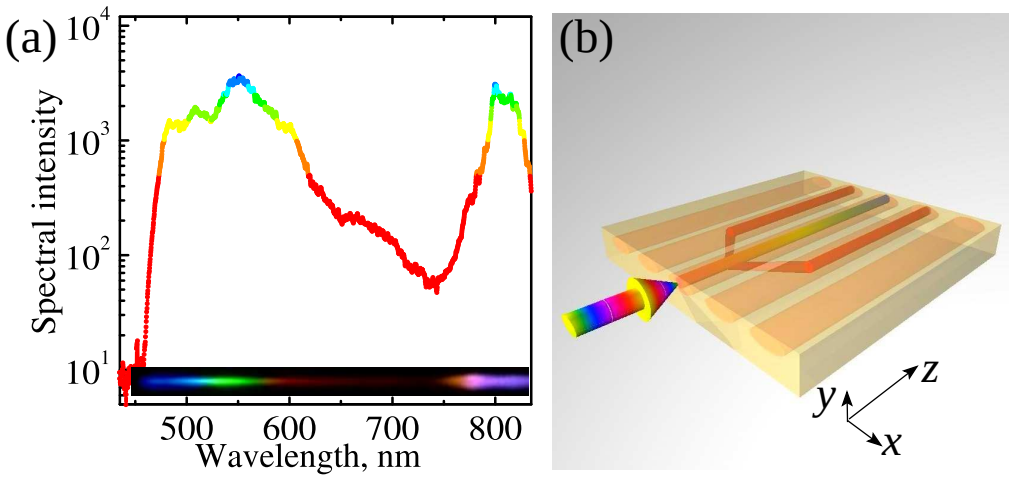

Fig. 4. (a) Spectrum of the generated supercontinuum radiation. (b) Schematic of the experiment showing the dispersion of the colors inside the array of optical waveguides [30].

3.4. Polychromatic breathers

A fundamentally different localization regime where the individual profiles of all spectral components oscillate periodically along the propagation direction has been predicted very recently [29]. It was previously demonstrated that dynamically oscillating multigap breathers can be generated by coherent laser light [50], and the breather's oscillation period depends both on the input excitation and the structure of the bandgap spectrum [51, 52]. Since the bandgap spectrum strongly depends on the wavelength, it remained an open question whether multigap polychromatic breathers can exist. The simulation results reported in Ref. [29] and presented in Fig. 3(a) demonstrate that self-focusing nonlinearity can act to synchronize the dynamical oscillations of all spectral components, creating a spatially localized state with the properties similar to those of monochromatic breathers. The oscillations occur due to the beating of modes from the total internal reflection and Bragg-reflection gaps, as shown in Fig. 3(b). A distinguishing feature of the polychromatic breathers is that the propagation constant difference between the modes from different band-gaps is exactly the same for all the spectral components, despite the wavelength dependence of the bandgap structure.

4. Experimental demonstrations of multi-color self-trapping

4.1. Experimental setup

Before discussing the further developments of other ideas on polychromatic light control and self-focusing, we describe how the nonlinear effects of polychromatic light reshaping and self-trapping can be realized and observed experimentally. The key for such experimental realization is the combination of periodic structure with a broadband nonlinear response and high-spatial coherence, high optical intensity polychromatic light with a broad frequency spectrum. The natural choice of such light source is provided by the effect of supercontinuum generation. In this process, spectrally narrow laser pulses are converted into the broad supercontinuum spectrum through several processes [1, 2], including self-phase modulation, soliton formation due to the interplay between anomalous dispersion and Kerr-nonlinearity, soliton break-up due to higher order dispersion, and Raman shifting of the solitons, leading to non-solitonic radiation in the short-wavelength range. Such supercontinuum radiation has proven to be an excellent tool for

#84756 - $15.00 USD Received 2 Jul 2007; revised 7 Sep 2007; accepted 7 Sep 2007; published 26 Sep 2007

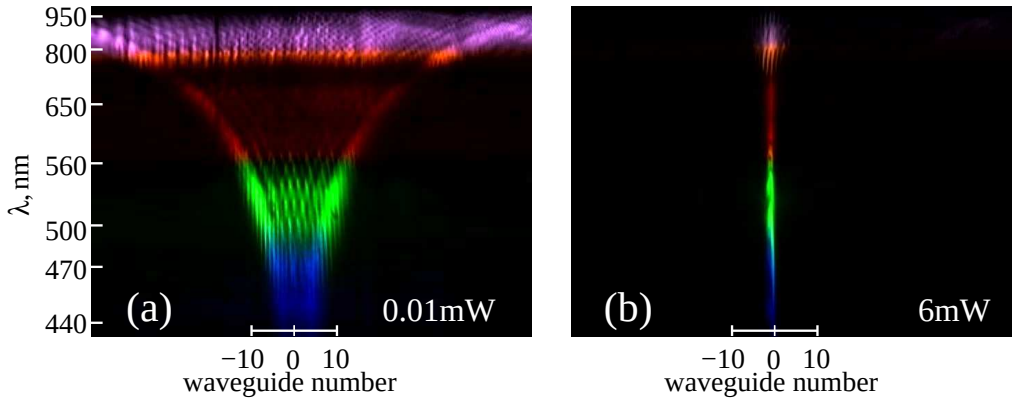

Fig. 5. Spectrally resolved measurements of the beam profiles at the output face of waveguide array ($d = 10\,\mu$m): (a) Polychromatic discrete diffraction at low laser power (0.01 mW), and (b) Nonlinear localization and formation of polychromatic gap soliton at a higher (6 mW) power [29, 32]. Movie: Temporal dynamics of the localization process, after the light was injected in the array.

characterization of bandgap materials [7], it possesses high spatial coherence [3], as well as high brightness and intensity required for nonlinear experiments [8]. In our experiments, we used a supercontinuum light beam generated by femtosecond laser pulses (140 fs at 800 nm from a Ti:Sapphire oscillator) coupled into 1.5 m of highly nonlinear photonic crystal fiber (Crystal Fiber NL-2.0-740 with engineered zero dispersion around 740 nm) [30]. The spectrum of the generated supercontinuum is shown in Fig. 4(a), and it spans over a wide frequency range (typically more than an optical octave). After re-collimation and attenuation, the supercontinuum is spectrally analyzed by a fiber spectrometer and is refocused by a microscope objective ($\times$20) to a single channel of a waveguide array [see Fig. 4(b)].

The optical waveguides are fabricated by indiffusion of a thin (100Å) layer of Titanium in an X-cut, 50 mm long mono-crystal lithium niobate wafer [21]. The waveguides are single-moded for all spectral components of the supercontinuum. Arrays with different periodicity and index contrast were tested in our experiments. An important property of the $LiNbO_3$ crystal is that it exhibits a nonlinear change of the optical refractive index at higher powers due to photorefraction [53, 54]. The photovoltaic nonlinearity [45] is of the defocusing type, meaning that an increase of the light intensity leads to a local decrease in the material refractive index.

After coupling to the array, its output is imaged by a microscope objective ($\times$5) onto a color CCD camera, where a dispersive 60° (glass SF-11) prism could be inserted between the imaging objective and the camera in order to resolve spectrally all components of the supercontinuum. Additionally, a reference supercontinuum beam is used for interferometric measurement of the phase structure of the output beam [32]. To compensate for the pulse delay and pulse spreading inside the $LiNbO_3$ waveguides, this reference beam is sent through a variable delay-line, implemented in a dispersion compensated interferometer, including an additional 5 cm long bulk $LiNbO_3$ crystal (to equalize the material dispersion). In this way, interferometric measurements are possible for ultra-wide spectral range.

4.2. Generation of polychromatic gap solitons

To obtain a detailed insight into the spectral distribution at the array output, we resolve the individual spectral components by a prism and acquire a single shot two-dimensional image providing spatial resolution in one (horizontal) direction and spectral resolution in orthogonal

#84756 - $15.00 USD Received 2 Jul 2007; revised 7 Sep 2007; accepted 7 Sep 2007; published 26 Sep 2007

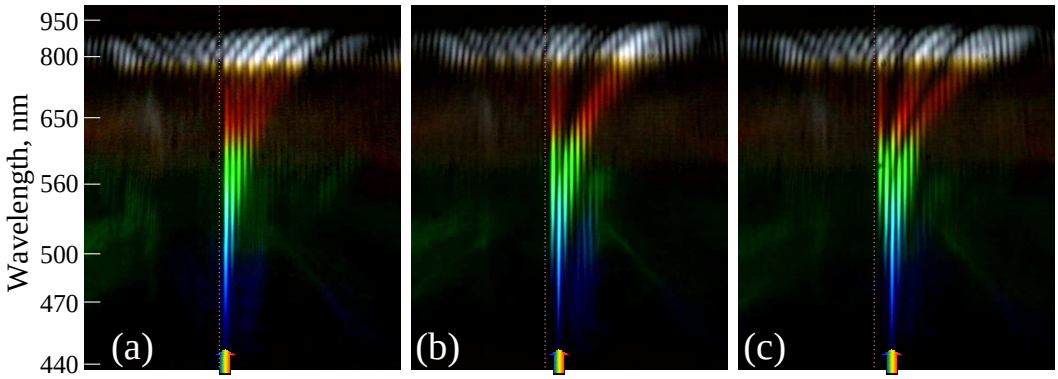

Fig. 6. Spectrally-resolved reflection and transmission of a low-power probe beam (0.01 mW) from an optically-induced defect when the array ($d = 19\,\mu$m) is probed (a) next to the defect; (b) one waveguide away; (c) two waveguides away [30].

(vertical) direction. This technique enables precise determination of the spectral distribution at the array output. The image in Fig. 5(a) depicts the spectrally resolved discrete diffraction of the supercontinuum beam in an array of optical waveguides with a period $d = 10\,\mu$m when the input beam is focused to a single waveguide. The diffraction of the beam is weakest for the blue spectral components, which experience weak coupling, while the diffraction is strongest for the infrared components. We note that the spectral scale in Fig. 5(a) is not linear due to the nonlinear dispersion of the prism. The spectrally resolved discrete diffraction provides a visual illustration of the separation of colors in the waveguide array. This separation occurs as the light is concentrated predominantly in the beam wings rather than in the center, a typical property of the discrete diffraction. The recorded diffraction patterns also allow for characterization of the linear dispersion of waveguide coupling and discrete diffraction. For the output pattern presented in Fig. 5(a), we find that the discrete diffraction length, defined as the characteristic distance where the diffraction pattern at the specific wavelength is expanded by two extra waveguides, varies from 1 cm, for blue (480 nm), to less than 0.2 cm, for red (800 nm) spectral components. These values correspond to a total propagation distance of 5.5 and 27.5 discrete diffraction lengths for the blue and red spectral components, respectively, in a 5.5 cm long waveguide array structure. The propagation of few diffraction lengths for all spectral components is advantageous for nonlinear experiments, e.g. formation of solitons [55, 56], and facilitates strong spectral transformations in the nonlinear regime.

An important next step towards spectral reshaping is the ability to suppress the diffraction-induced broadening and separation of spectral components through nonlinear beam self-action [32]. In experiment, we observe strong spatio-spectral localization of the supercontinuum light as its input power is increased [Fig. 5(b)]. A distinguishable characteristic of this localization process is the fact that it combines all wavelength components (from blue to red) of the supercontinuum spectrum and as such achieves suppression of the spatial dispersion in the nonlinear regime through the formation of a *polychromatic gap soliton*. The dynamics of the localization process can be seen in Fig. 5(movie) which presents the temporal evolution of the output after the beam is injected in the array. The slow time response of the photovoltaic nonlinearity allows for the simple visualization of this dynamics, revealing the combined transition of all spectral components from discrete diffraction to soliton formation.

Taking advantage of the high spatial coherence of the supercontinuum light, we have also performed white-light interferometric measurement of the localized output profile. The observed interference pattern reveals that the dominating spectral components in the adjacent waveguides

#84756 - $15.00 USD Received 2 Jul 2007; revised 7 Sep 2007; accepted 7 Sep 2007; published 26 Sep 2007

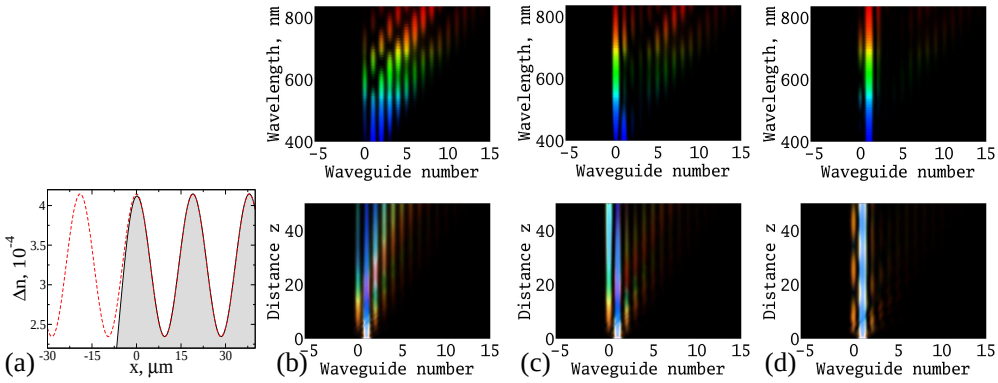

Fig. 7. (a) Refractive index profile in waveguide arrays with a surface defect. Dashed line shows, for comparison, the refractive index in an infinite periodic structure. (b) Numerically simulated linear and (c,d) nonlinear dynamics inside the array (bottom) and output spectra (top) for increasing powers of the input beam coupled to the second waveguide [27]. Simulations performed with $M = 50$ spectral components and defocusing nonlinearity ($\gamma = -1$).

are out-of-phase, providing confirmation that the localized beam is indeed a polychromatic gap soliton [29, 32]. We note that this type of localization is physically different from the gap solitons generated by two-color coupling in arrays with quadratic nonlinearity [17] where the second harmonic field has a plane phase in contrast to the staggered phase of the fundamental frequency component.

4.3. Interaction with an induced defect

A specific characteristic of the localization process in $LiNbO_3$ is the slow temporal response. The response time is inversely proportional to the input laser power, and it can vary from a few seconds to several minutes at low light intensities. The advantage of this slow time response, however, is that once the refractive-index modulation is written it can be preserved in the structure for a long period of time, provided that the sample is not exposed to strong light radiation [53]. This opens an exciting possibility for optical writing of defects with arbitrary geometry [54, 57, 58]. We demonstrate that defects can play a role of spectral filters for the supercontinuum light [30]. We generate a localized supercontinuum state in an array with periodicity of 19 μm at power of 12 mW and after several hours in a dark room we probe this induced defect with low power supercontinuum beam. When the light is injected into the waveguide adjacent to the defect [Fig. 6(a)] we observe reflection of all spectral components below a threshold wavelength value (approximately 800 nm in our case). On the other hand, only spectral components with longer wavelengths are transmitted to the left-hand side of the defect. When the input beam is injected into the second or third waveguide from the induced defect, we observe complex spectral reshaping of the output profiles due to the interference with waves reflected from the defect state. We note that the nonlinear refractive index change in the detuned waveguide is only of the order of 10^{-4}, but it is sufficient to modify significantly the spectrum of the supercontinuum radiation. This effect is somehow similar to surface manipulation of the supercontinuum light discussed below in Sec. 5, but with the ability for dynamical reconfiguration and all-optical tuning of the defect properties.

#84756 - $15.00 USD Received 2 Jul 2007; revised 7 Sep 2007; accepted 7 Sep 2007; published 26 Sep 2007

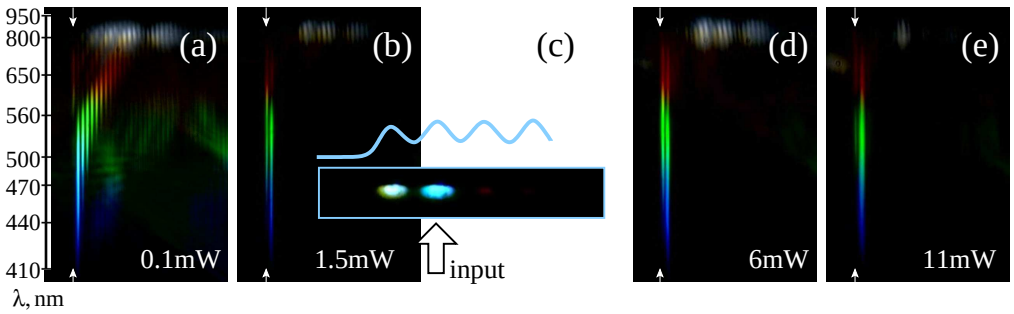

Fig. 8. Experimental demonstration of interaction with the surface defect of a supercontinuum polychromatic light beam coupled to the second waveguide. (a,b,d,e) Spectrally resolved spatial distributions at the output facet for increasing power levels. Arrows show the position of the surface waveguide. (c) Real-color output intensity distribution recorded with the CCD camera and schematic plot of the refractive index profile in the waveguide array [27].

5. Polychromatic nonlinear surface modes

In this section, we describe theoretically and demonstrate experimentally power-controlled reshaping of polychromatic light beams near the edge of the nonlinear waveguide array, and discuss additional possibilities for beam control at an interface between different lattices.

5.1. Spatial-spectral reshaping through nonlinear interaction with surface defect

Flexible control of light propagation in photonic lattices can be achieved when the optical beam interacts with the boundary of a periodic structure. By making the surface waveguide to be slightly different [see an example in Fig. 7(a)], it is possible to perform spectrally-selective control of linear waves. The surface defect can support localized guided modes when the refractive index change exceeds a certain threshold, such that the mode eigenvalue is shifted outside the photonic band [59, 60]. Since the bandgap structure of a photonic lattice depends strongly on frequency as discussed in Sec. 2, the critical change of the refractive index becomes also wavelength-dependent. Only when the optical wavelength is shorter than a certain threshold which depends on the strength of the surface defect, $\lambda < \lambda_{\text{th}}$, the optical waves can be localized at the surface [59, 60], whereas for longer wavelengths the light would be reflected from the surface experiencing modified discrete diffraction [61, 62]. For the refractive index profile shown in Fig. 7(a), the defect can trap blue spectral components whereas the longer wavelength components escape from the surface.

We have demonstrated [27] that by coupling light in the second waveguide, next to the surface defect, it is possible to perform power-dependent spatial-spectral reshaping. In the linear regime, the tunneling of short-wavelength components with $\lambda < \lambda_{\text{th}}$ to the first waveguide is suppressed almost completely. On the other hand, light at longer wavelengths can penetrate in the first waveguide, see Fig. 7(b). When the light intensity is increased, the refractive index at the location of the input beam keeps decreasing, approaching gradually the refractive index of the surface waveguide. When the mismatch between the two waveguides is reduced, shorter wavelength components start tunneling to the first waveguide. As this happens, nonlinearity acts to increase the mismatch, and light switches permanently to the first waveguide, as shown in Fig. 7(c). For even higher input powers, the refractive index of the second waveguide decreases to the values below the index of the neighboring waveguides, such that light remains trapped at the input location, see Fig. 7(d). The suggested method of beam manipulation was

#84756 - $15.00 USD Received 2 Jul 2007; revised 7 Sep 2007; accepted 7 Sep 2007; published 26 Sep 2007

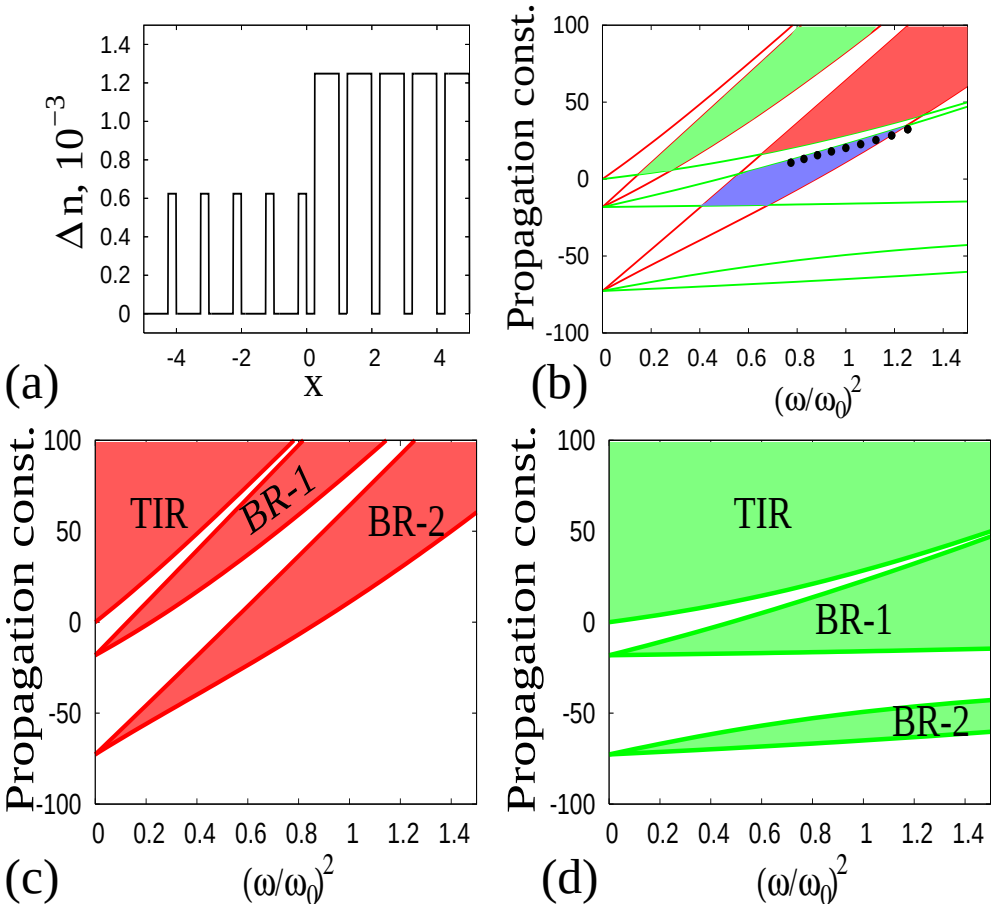

Fig. 9. (a) Refractive index profile at the interface of two waveguide arrays. (b) Edges of the spectral bands for the narrow waveguide array (green lines) and the wide waveguide array (red lines), and the overlap regions (red, green, and blue) vs. the light frequency scaled to ω_0 corresponding to 532 nm. (c,d) Individual band-gap spectra for the narrow and wide waveguide arrays, respectively. The total internal-reflection (TIR), first and second Bragg-reflection (BR) gaps are shown by shading [26].

also realized experimentally [27]. As the input power into the second waveguide is increased, we observe enhanced coupling of red, green, and blue components to the surface waveguide [Figs. 8(a-d)] and the formation of polychromatic surface modes. At even higher powers the second waveguide is fully detuned from the neighboring ones and we observe light trapping entirely in the second waveguide [Figs. 8(e)]. In the latter case, nonlinearity strongly reduces the influence of the surface on beam propagation. These results demonstrate that collective spatial switching of multiple spectral components can be realized through the nontrivial interplay between the effects of fabricated and self-induced nonlinear defects in photonic lattices.

5.2. *Polychromatic interface solitons*

Additional flexibility in tailoring beam shaping can be realized by introducing interfaces between two different lattices [25, 26, 63–65]. Such interfaces may support localized linear modes that generalize the so-called surface Tamm states known to exist in other similar structures

#84756 - $15.00 USD Received 2 Jul 2007; revised 7 Sep 2007; accepted 7 Sep 2007; published 26 Sep 2007

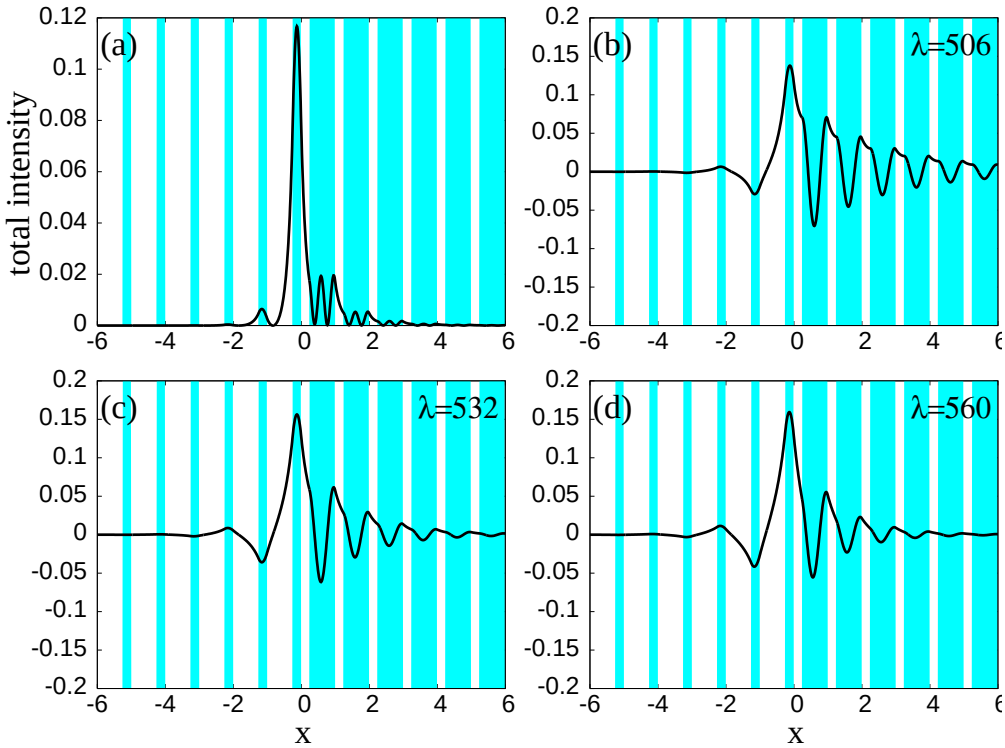

Fig. 10. Example of a polychromatic interface soliton consisting of five components of different wavelengths. Shown are (a) the total intensity and (b-d) amplitude profiles of three spectral components as indicated by labels [26].

for many decades. Nonlinear media allows for localization also in the cases when linear surface states are absent [61, 66–72]. Importantly, in both the linear and nonlinear regimes, the light can only be localized in the overlap between the spectral gaps of both lattices separated by an interface, see Fig. 9. We find that by tailoring wavelength dispersion of the individual lattice spectra it becomes possible to control the localization and diffraction of polychromatic beams [25, 26].

Figure 10 shows an example where the polychromatic interface soliton supported by *defocusing nonlinearity* is composed of five components with different wavelengths λ=506, 519, 532, 546, 560 nm (equidistantly spaced in frequency space) [26]. All five components carry the same power. In the soliton, the blue components have a larger spatial extent that the red ones. This is in a sharp contrast to other types of polychromatic solitons in infinite systems. Single components shown in Fig. 10 are located within the first spectral gap of the narrow waveguide lattice and the second gap of the wide waveguide lattice. We numerically studied the propagation of such multi-component solitons in the presence of an initial perturbation and did not observe any signs of instabilities at experimentally feasible propagation distances.

We have found that such solitons can be generated by a Gaussian beam injected at the narrow waveguide closest to the interface. The propagation constants of the generated polychromatic soliton are shown with circles in Fig. 9(b). The propagation constants are shifted due to negative nonlinearity into the first band-gap of the narrow lattice, however for the chosen frequency spectrum the localization is only possible at the overlap with the second gap of the wide lattice. The overlap vanishes for light of higher frequencies, and accordingly blue components are not localized at the interface [25, 26]. This effect is in sharp contrast to beam dynamics in bulk

#84756 - $15.00 USD Received 2 Jul 2007; revised 7 Sep 2007; accepted 7 Sep 2007; published 26 Sep 2007

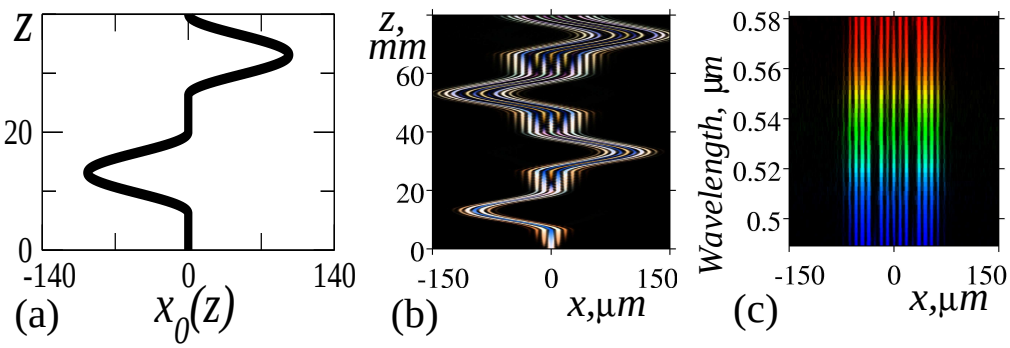

Fig. 11. Wavelength-independent diffraction in an optimized periodically curved waveguide array. (a) Waveguide bending profile with the period $L = 40mm$. (b) Calculated beam evolution inside the waveguide array. (c) Spectrally-resolved output profiles [28].

nonlinear media or periodic photonic lattices with cos-type refractive index modulation, where blue light does generally focus into solitons more easily than red light.

6. Broadband diffraction management in curved waveguides

The dependence of spatial beam diffraction on optical wavelength is a universal effect, which takes place both in free space [73] and in various types of photonic-crystal structures including photonic lattices as discussed in Sec. 2. We have demonstrated that intrinsic wavelength-dependence of diffraction strength in waveguide arrays can be compensated by introducing periodic waveguide bending in the longitudinal direction [28]. It was previously suggested that the longitudinal bending can be used to manage the diffraction strength [74–79], however the diffraction control was restricted to a spectral range of less than 10% of the central frequency. We found that with a special design of bending profiles, the wavelength-independent diffraction can be achieved in a very broad spectral range up to 50% of the central frequency. The periodic structures can be optimized to obtain constant normal, anomalous, or zero diffraction for polychromatic beams. Despite the transitional separation of colors inside the waveguide array, after each bending period all color components are recombined, as illustrated in Fig. 11. This opens up novel opportunities for efficient self-collimation, focusing, and shaping of white-light beams and patterns. The broadband diffraction control also enables the creation of efficient intergated nonlinear optical devices for switching of polychromatic light [80].

The optimized structures can also be used to manipulate white-light patterns through *multicolor Talbot effect*, which otherwise is not feasible in free space or in conventional photonic lattices. The Talbot effect [81] is known as the repetition of any periodic monochromatic light pattern upon propagation at certain equally spaced distances. It was recently shown that the Talbot effect is also possible in discrete systems for certain periodic input patterns [35], see an example in Fig. 12(a).

Period of the discrete Talbot effect in the waveguide array is inversely proportional to the coupling coefficient between waveguide modes, which strongly depends on frequency. Therefore, for each specific frequency Talbot recurrences occur at different distances [35], and periodic intensity revivals disappear for the multicolor input, see Fig. 12(b). Multicolor Talbot effect is also not possible in free space where the revival period is proportional to frequency. Most remarkably, multicolor Talbot effect can be observed in optimized waveguide arrays with wavelength-independent diffraction [28], see an example in Fig. 12(c).

It is important that the basic concept of the broadband diffraction management and control

#84756 - $15.00 USD Received 2 Jul 2007; revised 7 Sep 2007; accepted 7 Sep 2007; published 26 Sep 2007

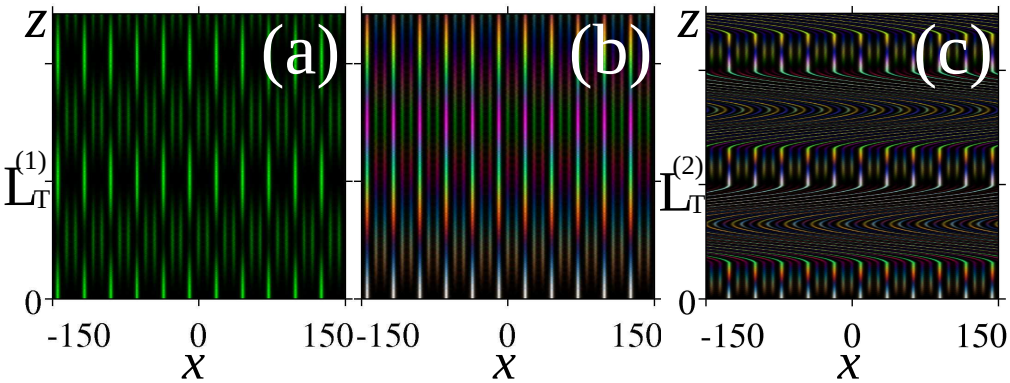

Fig. 12. (a) Monochromatic Talbot effect in the straight waveguide array: periodic intensity revivals every $L_T^{(1)} = 16.5mm$ of propagation for the input pattern $\{1,0,0,1,0,0,\ldots\}$ and the wavelength $\lambda_0 = 532nm$. (b) Disappearance of the Talbot carpet in the straight array when input consists of three components with equal intensities and different wavelengths plotted by different colors $\lambda_r = 580nm$ [red], $\lambda_0 = 532nm$ [green], and $\lambda_b = 490nm$ [blue]. (c) Multicolor Talbot effect in the optimized structure with wavelength-independent diffraction. Half of the bending period $L/2 = L_T^{(2)} = 53.2mm$ is equal to the Talbot distance for the corresponding effective coupling length [28].

can be extended to the case of *two-dimensional photonic lattices* composed of periodically-curved waveguides. Recently, we have suggested that a specific design of the waveguide bending would allow one not only to control both the strength and sign of light diffraction but also to *engineer the effective geometry and even dimensionality* of the photonic lattice [31]. In particular, we have demonstrated that different spectral components of polychromatic light beams can experience completely different types of diffraction, e.g. planar, triangular, or rectangular, in the same structure. These results provide a solid background for the further experimental studies of modulated photonic lattices, and they suggest novel opportunities for efficient reshaping of polychromatic light beams in two-dimensional photonic structures.

7. Conclusions

We have presented an overview of the basic theoretical studies and experimental observations of spatio-spectral control of polychromatic light in periodic photonic structures. For nonlinear lattices, we have described theoretically new types of self-trapped states in the form of rainbow gap solitons, polychromatic surface waves, and multigap breathers, all possessing nontrivial phase structure and spectral features. We have presented the first observation of polychromatic gap solitons in periodic photonic structures with defocusing nonlinearity; such solitons can be generated due to simultaneous spatio-spectral localization of supercontinuum radiation inside the photonic bandgaps. For linear photonic lattices, we have demonstrated that the strength of diffraction can be managed in optimized arrays of curved waveguides allowing an efficient diffraction management of polychromatic light and realization of multicolor Talbot effect, which is possible neither in free space nor in conventional photonic lattices. We anticipate that many of the theoretically predicted and experimentally demonstrated effects can be useful for tunable control of the wavelength dispersion for ultra-broad spectrum pulses offering additional functionality for broadband optical systems and devices.

#84756 - $15.00 USD Received 2 Jul 2007; revised 7 Sep 2007; accepted 7 Sep 2007; published 26 Sep 2007

Acknowledgments

We would like to thank our collaborators and research students for their substantial and valuable contributions to the results summarized in this review paper. Especially, we are indebted to J. Bolger, A. Dreischuh, B. J. Eggleton, R. Fischer, I. L. Garanovich, W. Krolikowski, A. Mitchell, and K. Motzek. The work has been supported by the Australian Research Council.